STUDIA UNIVERSITATIS BABEŞ-BOLYAI, CHEMIA, LII, 2, 2007

A DENSITY FUNCTIONAL STUDY OF AROMATIC RING OXYGENATION BY RIESKE DIOXYGENASE ACTIVE SITES. 2. ENERGETICS OF THE PROPOSED REACTION MECHANISMS

RADU SILAGHI-DUMITRESCU*

ABSTRACT. Density functional (DFT) calculations were performed on the non-heme mononuclear iron active site of Rieske dioxygenases (RDOs), on complexes of this site with dioxygen and activated oxygen species that have been implicated in the RDO catalytic cycle, and with the model substrate, benzene. The results were generally consistent with previous DFT studies on model compound and RDOs and recent crystal structures of dioxygen- and substrate-bound naphthalene dioxygenase., However, we identify alternative preferred pathways for substrate di-hydroxylation at the RDO active site and show, in contrast to a previous DFT study, that a formally perferryl ($[Fe(V)(O)(OH)]^{2+}$) species is a plausible intermediate in aromatic substrate di-hydroxylation. The intriguing possibility that RDOs use "controlled Fenton chemistry" to di-hydroxylate aromatic substrates is also addressed.

INTRODUCTION

Rieske dioxygenases (RDO) are non-heme iron enzymes catalyzing the *cis*-1,2 di-hydroxylation of aromatic substrates by molecular oxygen and a reductant (typically one of the reduced pyridine nucleotides (NAD(P)H), inserting the equivalent of hydrogen peroxide and resulting in a non-aromatic dihydrodiol. (see Scheme 1).

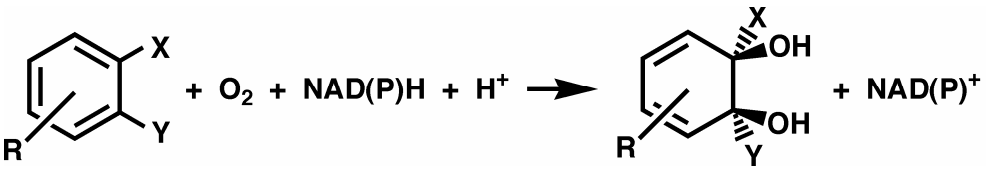

Scheme 1

* Department of Chemistry, "Babeş-Bolyai" University, Cluj-Napoca RO-400028, Romania

Mechanisms based on biochemical and model compound evidence proposed for the RDO-catalyzed reaction are shown in Figure 1.[1] In model compounds, ferric-hydroperoxo (Fe(III)-OOH) adducts are often found to undergo O-O bond cleavage forming higher-valent iron complexes (Fe(IV)=O, ferryl or Fe(V)=O, perferryl) with increased oxidative properties compared to the parent Fe(III)-OOH adducts.[1] While such chemistry is well-documented in heme enzymes, only one such high-valent intermediate has been identified in a non-heme iron oxygenase.[1] Of the ferrous-dioxygen, ferric-peroxo, ferric hydroperoxo and perferryl reaction intermediates proposed for RDOs, only the putative ferrous-dioxygen state of naphthalene dioxygenase (NDO) has been observed.[2]

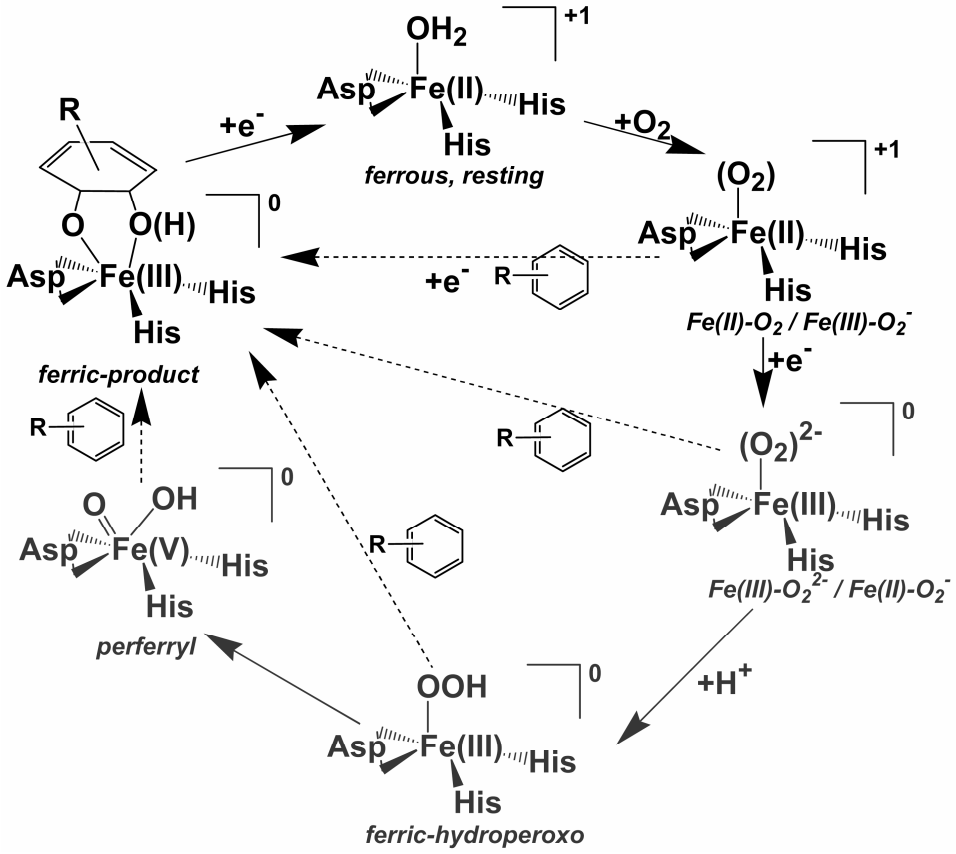

Figure 1. Proposed RDO catalytic mechanisms. Species shown in grey have never been observed in RDO. The identities of the protein-derived iron ligands are indicated. The aromatic substrate may be benzene (R = hydrogen), substituted benzenes, or other aromatics (including heterocyclic compounds).

Siegbahn and co-workers[3] recently reported a computational study on the mechanism of substrate oxidation by RDO, employing density functional theory (DFT). Their results indicated that this $S = 5/2$ ferric-hydroperoxo state would be capable of hydroxylating naphthalene in a multi-step mechanism where the highest activation barrier was 17-19 kcal/mol. O-O bond cleavage within $S = 5/2$ ferric-hydroperoxo [Fe(III)-OOH]$^{2+}$ was found to be prohibitively high, ~27 kcal/mol, suggesting that a perferryl-(oxo),hydroxo ([Fe(V)(O),OH]$^{2+}$) species would never form during the RDO catalytic cycle. O-O bond cleavage was calculated to be even more facile (activation barrier, 16 kcal/mol) in a ferrous-hydroperoxo model that would formally result upon one-electron reduction of ferric-hydroperoxo. The ferrous-hydroperoxo model was calculated to hydroxylate naphthalene in a stepwise mechanism where the highest activation barrier (involving initial attack on a carbon atom by the non-protonated oxygen atom of the Fe(III)-O-OH moiety) was 19 kcal/mol. A ferrous-hydroperoxo mechanism would be unprecedented in non-heme iron oxygenases; such chemistry is better known in heme enzymes and in non-heme model compounds.[4]

Prior to publication of Siegbahn and co-worker's DFT study,[3] we obtained an extensive set of data on the RDO catalytic cycle employing a slightly different computational strategy (BP86 functional vs. B3LYP, and a different choice of geometrical constraints on the protein-derived ligands). Our results are mostly, but not completely consistent with those of Siegbahn and co-workers.[3]. We report here the portion of our results that distinctly impacts our understanding of the RDO catalytic cycle. In particular, a substrate dihydroxylation pathway involving a perferryl-(oxo),hydroxo intermediate is shown to be feasible for RDO. A feasible mechanism for substrate hydroxylation by a Fe(II)-OOH intermediate is also identified, involving initial attack by the terminal -OH, which is distinct from that previously characterized by Siegbahn and co-workers. ZINDO/S-CI computed electronic absorption spectra are reported for proposed reaction intermediates, in an attempt to facilitate structure assignment upon UV-vis absorption spectra if/when such intermediates are characterized experimentally.

RESULTS AND DISCUSSION

Putative catalytic intermediates. The electronic structures of the putative intermediates illustrated in Figure 1, i.e. ferrous-dioxygen, ferric-peroxo, ferric-hydroperoxo and perferryl were previously described (accompanying article in this issue, and Ref[3]) and are not discussed here in detail,. We note that for

"ferrous-dioxygen" models our approach favours side-on vs. end-on geometries and $S = 5/2$ vs. $S = 3/2$, which is consistent with the experimentally-observed side-on dioxygen coordination in the NDO crystal structure.[2] The particularly long O-O bond observed experimentally (1.4 Å) is well reproduced.[2] For the perferryl intermediate, $S = 1/2$ is calculated to be the ground state, with an Fe(V)-type electronic structure consistent with previous descriptions. It is shown elsewhere that molecular orbitals and spin densities derived from DFT may be misleading in describing "high-valent" iron in biological coordination environments, and that more mundane Fe(III) or Fe(II) descriptions (with extra oxidizing equivalents localized on the ligands) are obtained with post-HF methods.[5,6]

In addition to the models already reported upon by Siegbahn and co-workers,[3] we also examined the effect of adding a water molecule to the coordination environments of ferrous-dioxygen, ferric-peroxo and ferric-hydroperoxo. Spectroscopic evidence for two water molecules in the iron coordination sphere exists in contrast to crystal structures showing only one water molecule.[2,7,8] The added water molecule did not alter the electronic structures and in particular the general preference for high-spin states and side-on coordination of O_2 and O_2^{2-}; This lack of effect together with the long iron-water bond seen in the most stable isomers, argue against a key role of a water ligand in controlling electronic structure.

O-O bond cleavage. Siegbahn and co-workers previously calculated a 26 kcal/mole activation barrier for O-O bond cleavage in an $S = 5/2$ ferric-hydroperoxo RDO model which was deemed to be prohibitively high.[3] Figure 2 shows the calculated energy profile for O-O bond elongation and cleavage in our $S = 5/2$ Fe(III)-OOH model. Consistent with previous results, the process is endothermic. In contrast to the previous results, however, the significantly lower estimated activation barrier of 15.9 kcal/molimplies that at O-O bond cleavage from this species is feasible. The product's $S = 3/2$ and $S = 1/2$ states are 7-30 kcal/mol (depending on conformer and spin state) more stable than $S = 5/2$, implying that O-O bond cleavage would be feasible both kinetically and thermodynamically. In fact, a lowering of the right-hand side of the diagram in Figure 2 by 30 kcal/mol implies that the activation barrier may well be lower than 15 kcal/mol – and thus even more feasible.

The reaction coordinate driving process illustrated in Figure 2 is expected to be sensitive to minor changes in starting geometry, the geometrical coordinate chosen, and the method used in following that

geometry. For the results in Figure 2, the O-O bond was elongated stepwise from the equilibrium distance of 1.46 Å in $S = 5/2$ ferric-hydroperoxo, $[Fe(III)\text{-}OOH]^{2+}$, to 2.36 Å in $S = 5/2$ perferryl-(oxo)hydroxo, $[Fe(V)(O)(OH)]^{2+}$; the geometry optimized at an O-O distance of {1.46 + n} Å ($n \geq 0.10$) is used as starting point for geometry optimization at {1.46 + n + 0.10} Å (with smaller steps at higher energies). An alternative to this process would be to vary the Fe---OH distance, as it changes from 2.36 Å in $S = 5/2$ $[Fe(III)\text{-}O\text{-}OH]^{2+}$ to 1.82 Å in $S = 5/2$ $[Fe(V)(O)(OH)]^{2+}$. However, this latter approach failed to identify a plausible O-O cleavage mechanism: stepwise shortening of the Fe-OH distance down to 1.82 Å was found not to bring about *any* elongation in O-O bond length, and removal of the Fe-OH constraint invariably resulted in the structure converging back to the Fe(III)-OOH starting geometry. This difference between two approaches for monitoring the same reaction caution us for further studies and is also likely to at least partially explain the difference between our results and those of Siegbahn and co-workers.[3] Further differences are expected to arise from the different treatment of the model; to mimic steric constraints imposed by the protein, Siegbahn and co-workers included in their models the □-carbon atoms of the histidine ligands and then froze the positions of these two carbon atoms as well as the position of the acetate methyl carbon.[3] However, having noted that free movement of the carboxylate in our models invariably results in a quasi-symmetrical bidentate coordination of the acetate to the iron (unlike in *any* of the RDO crystal structures), and having noted that significant rotation and reorientation of the imidazole rings occur upon unconstrained geometry optimization, we chose to freeze the positions of *all* protein-derived heavy atoms, allowing free movement of the iron, protons, and exogenous ligands.

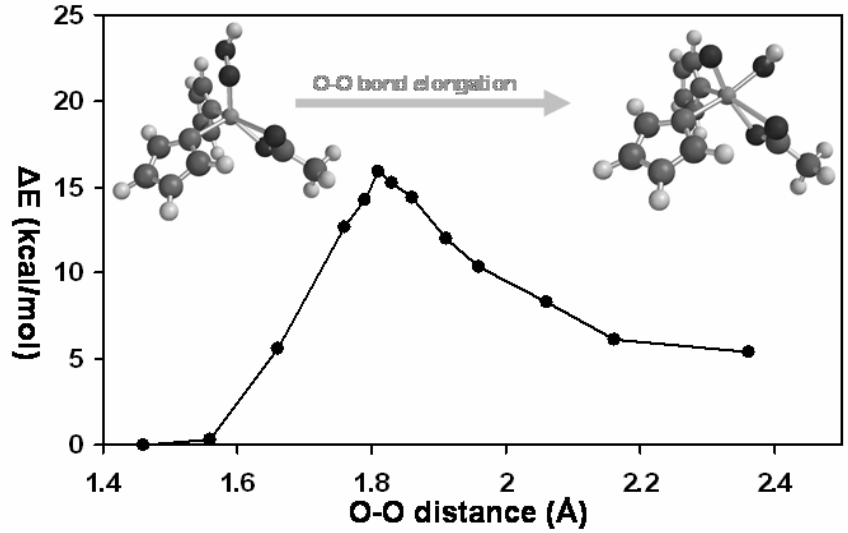

Figure 2. Variation of the potential energy as a function of the O---O distance during O-O bond cleavage within a *S* = 5/2 [Fe(III)-OOH]$^{2+}$ model (structure shown on the left), to yield *S* = 5/2 [Fe(V)(O)(OH)]$^{2+}$ (structure shown on the right).

Substrate di-hydroxylation. Figures 3 and 4 illustrate possible processes leading from an RDO reaction intermediate to di-hydroxylated product. The ferric-hydroperoxo (B) and perferryl-(oxo)hydroxo species (D and E) were the most likely candidates based on model compound studies.[3] The ferric-peroxo state (F) was also previously proposed.[2] Concerted as well as stepwise mechanisms are considered. Benzene, the simplest aromatic RDO substrate, is used in these calculations. Previous calculations by Siegbahn and co-workers employed a larger substrate, naphthalene, which is intrinsically expected to show slightly lower activation barriers than benzene.[9]

We identified one pathway (E) for benzene di-hydroxylation with a low activation barrier (11 kcal/mol) involving a perferryl, [Fe(V)(O)OH]$^{2+}$, as the di-hydroxylating agent. Although previous computational studies of synthetic complexes had suggested the feasibility of perferryl formation form ferric-hydroxperoxo,[10,11] Siegbahn and co-workers reported that di-hydroxylation of naphthalene was more likely to occur directly from a ferric-hydroperoxo with a lowest activation barrier of 17.5 kcal/mol.[3] Our results, on the other hand, indicate that the barrier for di-hydroxylation by [Fe(III)-OOH]$^{2+}$ (22 kcal/mol) is higher than the barrier for O-O bond cleavage in [Fe(III)-OOH]$^{2+}$ (16 kcal/mol).

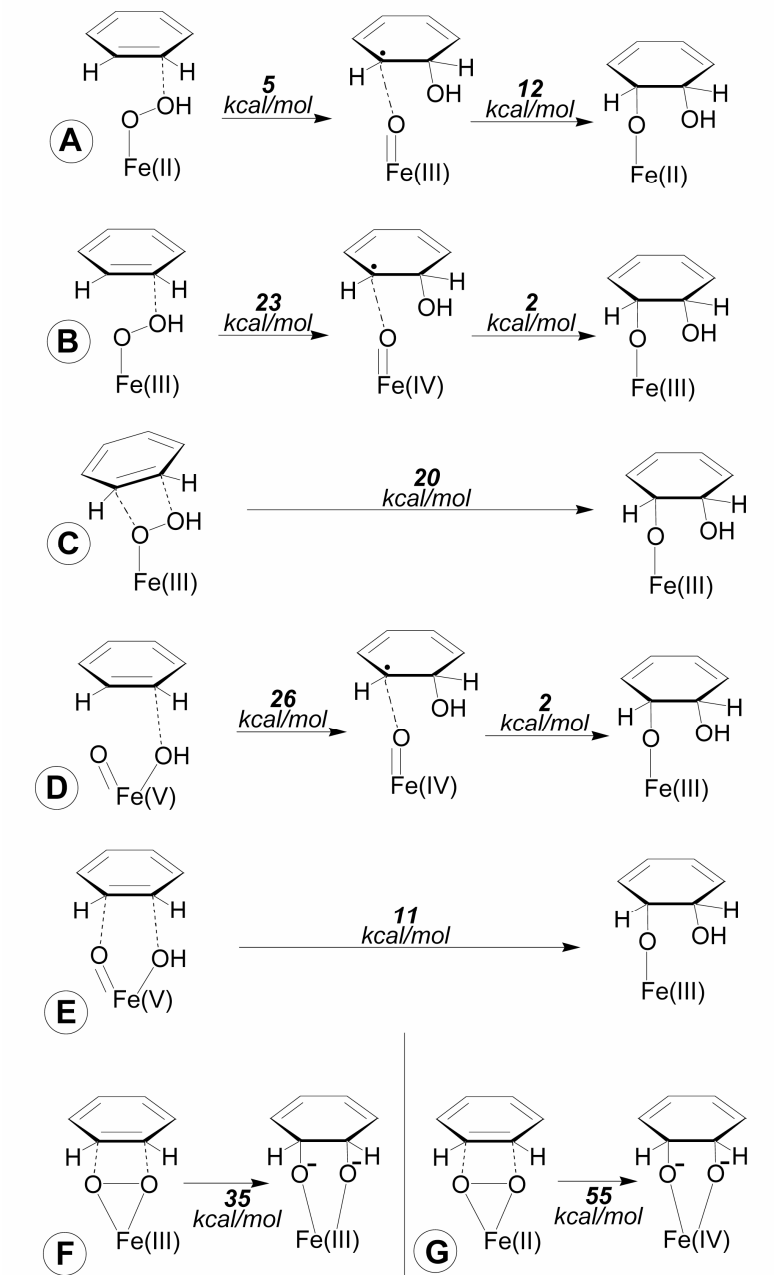

Figure 3. Possible mechanisms for substrate di-hydroxylation by RDO. Numbers indicate estimates of activation barriers based on data shown in Figure 4.

As did Siegbahn and co-workers,[3] we found a ferrous-hydroperoxo, $[Fe(II)\text{-}OOH]^+$, model to be an even lower-activation-barrier di-hydroxylating agent. We, thus, find that the pathway involving facile transfer of an OH radical-like moiety from Fe(II)-O-OH to substrate has a lower activation barrier than the pathway reported by Siegbahn and co-workers, which involved initial O-O bond cleavage of ferrous-hydroperoxo, $[Fe(II)\text{-}O\text{-}OH]^+$, to formally ferryl, $[Fe(IV)(O)(OH)]^+$, followed by substrate di-hydroxylation, with both steps relatively feasible energetically. Our lower estimated activation barrier, 12 kcal/mol, may relate to the fact that our calculated equilibrium O-O distance in $[Fe(II)\text{-}OOH]^+$ is extremely long (1.9 Å) even in the absence of the substrate, implying that substrate hydroxylation by this ferrous-hydroperoxo does not incur an additional energy penalty for breaking an O-O or Fe-O bond. Based on the computed activation barriers, Fe(III)-peroxo (reactions B and C in Figure 3) and Fe(II)-dioxygen (reaction G in Figure 3) are found significantly less likely to be involved in substrate hydroxylation.

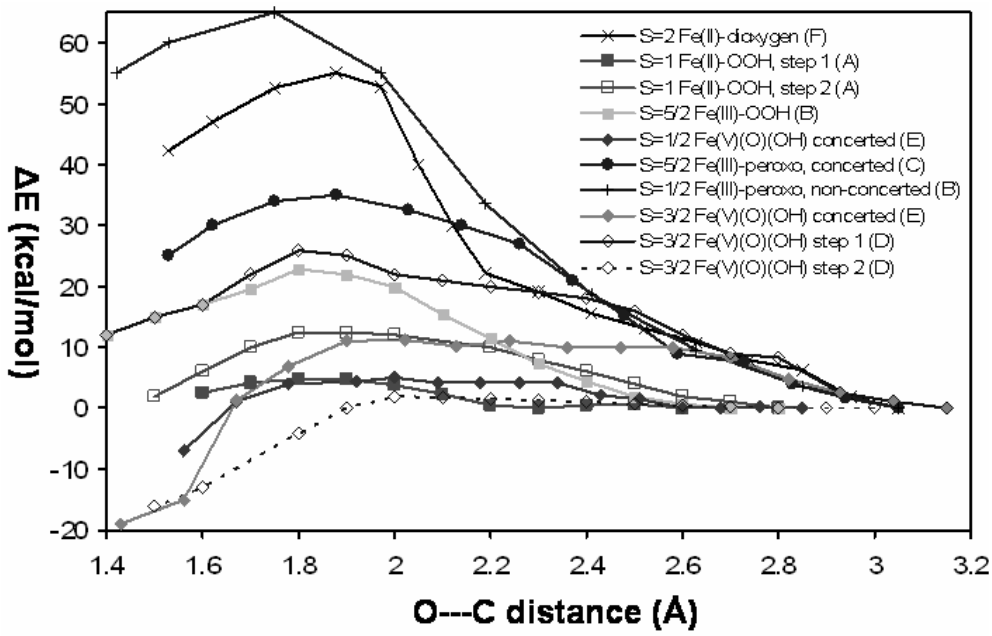

Figure 4. Variation of the potential energy as a function of the O---C distance(s) during substrate hydroxylation for the structures shown in Figure 3.

Figure 5 illustrates the overall calculated thermodynamics of dioxygen activation by the RDO model employed in the present study. The first step, reduction of the resting Fe(III) state, is extremely favorable thermodynamically. The high electron affinity calculated for the "resting" Fe(III) RDO is consistent with the fact that this state has never been observed experimentally; RDOs are typically isolated in the ferrous state even under aerobic conditions.[12,13] Similarly, the high electron affinity of the ferrous-dioxygen state (136 kcal/mol,) is suggestive of a very short lifetime. The extremely elongated O-O bond (1.36 Å) in the formally $[Fe(II)\text{-}O_2]^{2+}$ RDO, suggestive of a partial Fe(IV)-peroxo character, may contribute to the high electron affinity; the increased reactivity suggested by the strained O-O ligand in the ferrous-dioxygen adduct is however not enough by itself to support substrate hydroxylation (cf. Figures 3 and 4, the barrier would be 55 kcal/mol). The putative ferrous-dioxygen state has been observed experimentally only in a NDO crystal structure, where the exact oxidation state of the mononuclear site could not be probed; one-electron reduction to $Fe(III)\text{-}O_2^{2-}$ cannot be excluded;[2] according to our DFT results, the ferrous-dioxygen and ferric-peroxo states would be geometrically indistinguishable by protein X-ray crystallography at typical resolutions of 1.7-2.5 Å. The proton affinity of the ferric-peroxo state, ~250 kcal/mol, is somewhat lower but still in the same range as the proton 330-430 kcal/mol proton affinities of ferric-peroxo adducts of hemoproteins calculated at the same level of theory;[14] the hemoprotein ferric-peroxo adducts become protonated even at temperatures significantly below 0^{o} C, again suggesting a short lifetime for ferric-peroxo RDO. From the ferric-hydroperoxo stage, product can be formed either directly as proposed by Siegbahn and co-workers,[3] or via a perferryl intermediate; the activation barriers for these processes are in the range 11-17 kcal/mol, which is the same range seen for substrate hydroxylation by cytochrome P450 Compound I at the same level of theory.[15-18] With P450 Compound I eluding observation in the presence of substrate even at cryogenic temperatures,[19] isolation/detection of an RDO hydroxylating intermediate is expected to be similarly challenging experimentally.

The emerging picture from the present results and those of Siegbahn and co-workers[3] is that aromatic substrate di-hydroxylation at the RDO active site is feasible with ferric-hydroperoxo as well as perferryl intermediates, with our results suggesting that the latter is slightly preferred, and that a ferrous-hydroperoxo, $[Fe(II)\text{-}OOH]^{+}$, species – if ever formed - would be the lowest-activation-barrier hydroxylating agent of all

those considered here. This very reactive $[Fe(II)OOH]^+$ species with a long O-OH bond is reminiscent of the "bound hydroxyl radical" characterization of the Fenton reagent.D. T. Sawyer, A. Sobkowiak, T. Matsushita, *Acc. Chem. Res.*, 1996**, 29**, 409. While the possibility that RDOs use "controlled Fenton chemistry" to di-hydroxylate aromatic substrates is intriguing, there is currently no evidence for formation of ferrous-(hydro)peroxo species in Rieske dioxygenases. RDO active sites may actually be designed to *avoid* formation of a ferrous-hydroperoxo, since its high reactivity would make it less selective in its targets. More reliable computational results would likely emerge from QM/MM calculations directly accounting for the protein environment. However, the issue of locating a suitable pathway for the various reactions (as exemplified by the differences between our results and those of Siegbahn and co-workers) would not necessarily be alleviated by use of a larger model. These theoretical approaches can, nevertheless, complement and guide ongoing attempts to trap the actual intermediates in the RDO catalytic cycle.

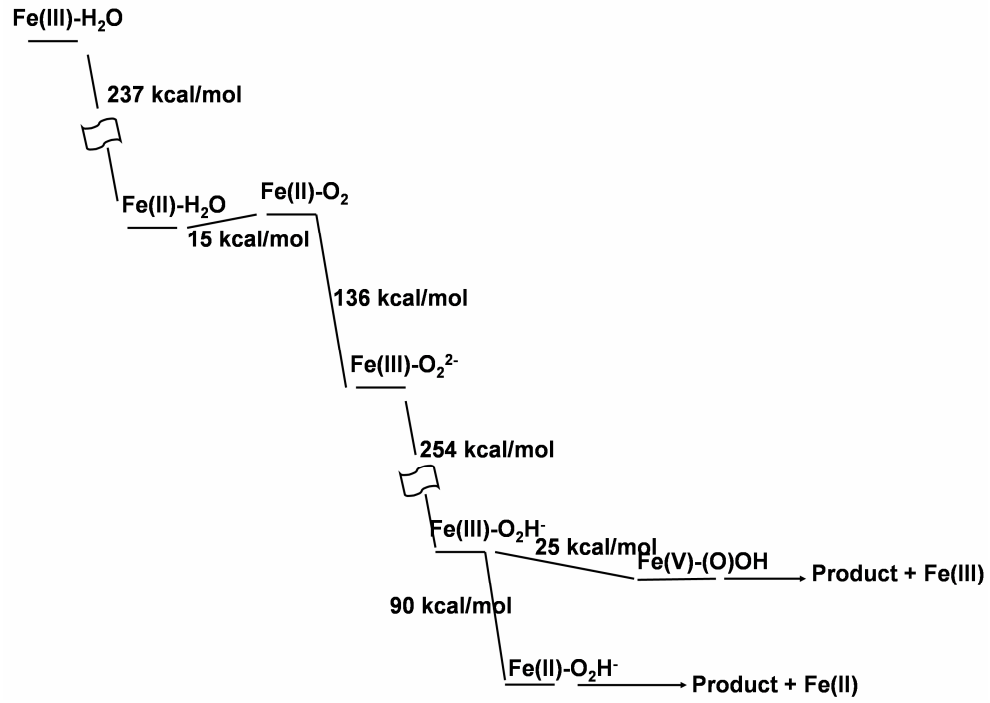

Figure 5. DFT-derived thermodynamics of dioxygen activation by RDO.

METHODS

The BP86 functional, which uses the gradient corrected exchange functional proposed by Becke (1988)[20] and the correlation functional by Perdew (1986),[21] and the DN** numerical basis set (comparable in size to 6-31G**) were used as implemented in *Spartan*.[22] For the SCF calculations, a fine grid was used and the convergence criteria were set to 10^{-6} (for the root-mean square of electron density) and 10^{-8} (energy), respectively. For geometry optimization, convergence criteria were set to 0.001 au (maximum gradient criterion) and 0.0003 (maximum displacement criterion). Charges and spin densities were derived from Mulliken population analyses after DFT geometry optimization.

Active site models were built using heavy-atom coordinates from Protein Data Bank entry 1EG9 (NDO with indole bound at the active site, 1.60 Å resolution). All models were constructed within the Builder module of the *Spartan* package. All models contained iron ligated by three protein-derived ligands: a carboxylate (modelled as CH_3COO^-) and two protonated (neutral) imidazoles (cf. Figure 2). The "fourth" (or fifth, if one counts the carboxylate as bidentate) ligand was water, peroxo, hydroperoxo, etc. For selected models, an extra water ligand was introduced in addition to the dioxygen/superoxo/peroxo ligand.

Reaction path calculations were set up starting from the separately calculated structures of ferrous-dioxygen, ferric-peroxo, ferric-hydroperoxo, ferrous-hydroperoxo and perferryl intermediates, to which a benzene moiety was added in such a way that each of the two iron-bound oxygen atoms was within 2.85 Å of a benzene carbon atom. The benzene moiety was placed above the His208 imidazole (using the residue numbering of the NDO crystal structure (the N1 imidazole in Figure S1, cf. Supporting Information), and roughly perpendicular to the Fe-O-O plane, so as to avoid placing the benzene hydrogens directly in between the oxygen and carbon atoms. To model a concerted mechanism, the two oxygen-to-carbon distances were constrained to be equal to each other and with values varying monotonically in-between 2.85 and 1.3 Å. Alternatively, to model non-concerted mechanisms, only one oxygen-carbon distance was varied at a time. For monitoring cleavage of the O-OH bond in ferric-hydroperoxo models in the absence of benzene, the O-O distance was constrained, successively, to values ranging from the equilibrium distance in Fe-O-OH to the equilibrium distance in the perferryl-oxo-hydroxo isomer.

The orientation of the protein-derived ligands changed dramatically upon unconstrained geometry optimization. These changes included reorientation of the carboxylate from semi-bidentate to clearly (symmetrically) bidentate, and rotations of the imidazole rings. Due to constraints imposed by the protein, such changes are unlikely to be allowed at the RDO active site (nor is there any experimental evidence for them), and attempts were made to avoid them. One option was to constrain iron-ligand bond distances. However, this study attempts to examine and compare energies for various spin/oxidation states of putative reaction intermediates. Constraining iron-ligand bond distances to the values seen in the crystal structure might artificially favor certain iron oxidation and/or spin states. Therefore, all protein-derived heavy atoms were kept frozen upon geometry optimization, in all models, whereas, the iron and the exogenous ligands (water, oxygen, peroxide, etc.), as well as all hydrogen atoms, were not frozen upon geometry optimization. This approach allowed the iron-ligand distances to adjust in each model to a satisfactory degree, accommodating well any changes in spin/oxidation state. We note the non-octahedral environment around the iron, i.e., the ligands are not directly *trans* to each other, so that movement of the iron away or towards any one particular ligand does not necessarily affect other iron-ligand distances.

ACKNOWLEDGEMENTS

Dr. I. Silaghi-Dumitrescu (UBB) is thanked for helpful discussions.

REFERENCES

1. M. Costas, M. P. Mehn, M. P. Jensen, L. J. Que, Chem. Rev., 2004, **2**, 939.
2. A. Karlsson, J. Parales, R. Parales, D. Gibson, H. Eklund, Science, 2003, **299**, 1039.
3. A. Bassan, M. R. Blomberg, P. E. Siegbahn, J Biol Inorg Chem, 2004, **9**, 439.
4. R. Silaghi-Dumitrescu, Arch. Biochem. Biophys., 2004, **424**, 137.
5. R. Silaghi-Dumitrescu, Studia Univ. Babes-Bolyai, Chemia, 2005, **50**, 17.
6. V. Balland, M. F. Charlot, F. Banse, J. Girerd, T. A. Mattioli, E. Bill, J. F. Bartoli, P. Battioni, D. Mansuy, Eur. J. Inorg. Chem., 2004, 301.

7. T.-C. Yang, M. Wolfe, M. B. Neibergall, Y. Mekmouche, J. D. Lipscomb, B. M. Hoffman, J. Am. Chem. Soc., 2003, **125**, 2034.

8. T. C. Yang, M. D. Wolfe, M. B. Neibergall, Y. Mekmouche, J. D. Lipscomb, B. M. Hoffman, J Am Chem Soc, 2003, **125**, 7056.

9. A. Bassan, M. Blomberg, P. Siegbahn, L. J. Que, J. Am. Chem. Soc., 2002, **124**, 11056.

10. A. Bassan, M. R. Blomberg, P. E. Siegbahn, L. Que, Jr., J Am Chem Soc, 2002, **124**, 11056.

11. A. Bassan, M. R. Blomberg, P. E. Siegbahn, L. Que, Jr., Angew Chem Int Ed Engl, 2005, **44**, 2939.

12. D. M. Eby, Z. M. Beharry, E. D. Coulter, D. M. Kurtz, Jr., E. L. Neidle, J. Bacteriol., 2001, **183**, 109.

13. Z. M. Beharry, D. M. Eby, E. D. Coulter, R. Viswanathan, E. L. Neidle, R. S. Phillips, D. M. Kurtz, Jr., Biochemistry, 2003, **42**, 13625.

14. R. Silaghi-Dumitrescu, I. Silaghi-Dumitrescu, Rev. Roum. Chim., 2004, **3-4**, 257.

15. R. Silaghi-Dumitrescu, C. E. Cooper, Dalton Trans., 2005, 3477.

16. V. Guallar, M. H. Baik, S. J. Lippard, R. A. Friesner, Proc. Natl. Acad. Sci. USA, 2003, **100**, 6998.

17. V. Guallar, R. A. Friesner, J. Am. Chem. Soc., 2004, **126**, 8501.

18. B. Meunier, S. P. de Visser, S. Shaik, Chem Rev, 2004, **104**, 3947.

19. B. M. Hoffman, Acc. Chem. Res., 2003, **36**, 522.

20. A. D. Becke, Phys. Rev., 1988, 3098.

21. J. P. Perdew, Phys. Rev., 1986, **B33**, 8822.

22. Spartan 5.0, Wavefunction, Inc., 18401 Von Karman Avenue Suite 370, Irvine, CA 92612 U.S.A.